Article

Bi-modified Pt electrodes towards glycerol electrooxidation in alkaline solution: effects on activity and selectivity

Matheus Batista Cordeiro de Souza, Rafael Alcides Vicente, Victor Yoiti Yukuhiro, Cléo Thomás Gabriel Vilela Menegaz Teixeira Pires, William Cheuquepán, José Luiz Bott Neto, Jose Solla-Gullon, and Pablo S. Fernandez

ACS Catal., **Just Accepted Manuscript** • DOI: 10.1021/acscatal.9b00190 • Publication Date (Web): 08 Mar 2019

Bi-modified Pt electrodes towards Glycerol Electrooxidation in Alkaline solution: effects on Activity and Selectivity

Matheus B.C. de Souza[a], Rafael A. Vicente[a], Victor Y. Yukuhiro[a], Cléo T.G.V.M.T. Pires[a], William Cheuquepán[b], José L. Bott-Neto[a], José Solla-Gullón[b], Pablo S. Fernández[a*].

[a]Chemistry Institute, State University of Campinas, PO Box 6154, 13083-970, Campinas SP, Brazil.
[b]Instituto de Electroquímica, Universidad de Alicante, Apartado 99, 03080 Alicante, Spain.

ABSTRACT: Herein we investigate the effect of irreversibly adsorbed bismuth on polycrystalline platinum (Pt_p) on the electrooxidation of glycerol in alkaline media by combining electrochemical, spectroscopic (*in situ* FTIR) and analytical (HPLC *on line*) techniques. We found that the activity of Pt_p increases by about fivefold when the optimal quantity of Bi ions is added to the solution. Besides, the adatom strongly impacts the reaction products by suppressing the pathways with C-C bond breaking, hindering the formation of CO (and other unknown intermediates) and enhancing the production of Glycerate.

Different to the results in acid media for Pt_p-Bi systems where Bi block the oxidation pathway through the primary carbon, glycerate is the main product in alkaline media and dihydroxyacetone is either produced in extremely low quantities or not produced. Besides, comparing our results with those in acid media, the peak current recorded at 1 $mV.s^{-1}$ in this work was one order of magnitude higher. These results show the strong impact of the pH in the reaction rate and selectivity.

.KEYWORDS.Glycerol Electro-oxidation Reaction, Platinum, Bismuth, in situ FTIR, HPLC on line.

INTRODUCTION

The necessity for greener sources of energy has increased the biodiesel production around the world and generated a surplus of glycerol (GlOH), which is a byproduct of the biodiesel production.[1] Thus, the need for new application of GlOH motivated scientists from many fields to work in this direction.[2–5] In this context, the electrooxidation of GlOH (EOG) aroused as a possibility to use this molecule in anodes of: i) Fuel Cells: with the main aim of generating electric energy and ii) Electrolyzers: for the concomitant generation of oxidation products of GlOH with high value (in the anode)[1] and high purity hydrogen (in the cathode).[3,4]

Many papers have been published about EOG in noble metal-based electrodes,[6] mainly in acidic media and using carbon (or oxide) supported nanoparticles (NPs). However, there is still a lack of knowledge about the relation between the catalyst composition and structure with their activity, and the effect of the reaction selectivity, even for the most studied systems.

Although we will focus in works performed with bulk, non-supported materials, it is worth to mention several papers using NPs that motivated us to develop this work. The group of Coutanceau used carbon supported Pt, Pd, PtBi, PdBi and PtPdBi NPs and *in situ* FTIR experiments to study the EOG in alkaline media.[7,8] They observed the same reaction pathways for all the catalyst but the reaction selectivity depends on the electrode potential. Besides, long term electrolysis and HPLC analysis showed that the main reaction products were glycerate, dihydroxyacetone (DHA) and tartronate at low potentials. At potentials higher than 0.8V they detected oxalate and formate. The same group modified shape-controlled Pd NPs (spheres, cubes and octahedrons) with Bi[9] and studied the EOG in alkaline media. Electrochemical results did not show very significant changes with the addition of Bi, however, *in situ* FTIR showed modifications in the reaction pathways. Kwon et. al. showed that in acid solutions, the activity and selectivity of Pt/C NPs towards the EOG can be tuned by modifying the electrode with p-block adatoms.[10,11] Interestingly, they found that the modification with Sb[10] and Bi[11] promotes the electrooxidation of the secondary carbon producing DHA. Similar results have been obtained in heterogeneous catalysis.[12] Other adatoms (Sn, In, Pb) enhance the electrode activity by promoting the oxidation of the primary carbon, yielding glyceraldehyde and glyceric acid. Also, in acidic media, Caneppele et. al. showed that the modification of Pt/C NPs with Sb exponentially improves the activity towards the EOG.[13]

By modifying Pt single crystals with Bi in acidic media, Garcia et. al., showed that Bi enhances the EOG rate and the production of DHA in Pt(111). On the other hand, Bi adatoms lowered the Pt(100) activity and did not change the selectivity of the reaction in this surface.[14]

As observed for many small organic molecules, the current density for the EOG on Pt electrodes is an order of magnitude higher in alkaline than in acidic media.[15–17] Thus, in this work, we modified a polycrystalline Pt electrode (Pt_p) with different coverages of Bi and studied the catalyst activity and the reaction selectivity in alkaline media. By coupling electrochemical techniques to FTIR and HPLC *on line*, we obtained new insights about the effect of Bi adatoms towards the EOG in alkaline media. We found that the activity of Pt_p increases by about fivefold when the optimal quantity of Bi ions is added to the solution. Besides, the adatom strongly impacts the reaction products by suppressing the pathways with C-C bond breaking, hindering the formation of CO (and other unknown intermediates) and enhancing the production of glycerate.

In acid media, Bi blocks the oxidation pathway through the primary carbon,[11,14] generating DHA. In contrast, in alkaline media the adatom enhances the production of glycerate and DHA is either produced in low quantities or not produced. Regarding the activity of Pt_p-Bi, the peak current at 1$mV.s^{-1}$ in this work was one order of magnitude higher than that obtained in acid media.

EXPERIMENTAL SECTION

Electrochemical system and surface preparation.

A standard three-electrode cell and potentiostat/galvanostat (Autolab PGSTAT101, Methrom®) were used in all the experiments. The working electrode (WE) was Pt_p, consisting of a

Pt wire with a spherical ending. A Pt foil was used as counter electrode and the reference electrode was a reversible hydrogen electrode (RHE). All potentials mentioned in this work are referred to the RHE scale. The WE were cleaned by immersion in aqua regia for 30 s, rinsed with ultrapure water and flame annealed, followed by quenching in ultrapure water.

Irreversible adsorption of Bi on Pt was performed by immersion of the WE in an acidic Bi_2O_3 solution with concentrations ranging from 10^{-3} to 10^{-5} mol.L^{-1} at open circuit potential.[18] After rinsing with ultrapure water, the WE was transferred to an electrochemical cell containing a solution 0.1 mol.L^{-1} NaOH, and a blank voltammogram was recorded in a potential window from 0.05 to 0.45 V. The electrode coverage (θ_{Bi}) was calculated from the decrease in the hydrogen desorption peaks, after a stable voltammogram was obtained. The partially covered Pt electrode was then removed from the electrolyte solution at a fixed potential and transferred to another electrochemical cell containing a solution of 0.1 mol.L^{-1} NaOH + 0.1 mol.L^{-1} of GlOH. The modified Pt_p electrode will be called Pt_p-Bi from now on.

A Bi electrode was made by depositing high amounts of Bi on a polycrystalline Au electrode with a spherical end. Metallic Bi was deposited by applying a constant potential (-2 V) between the Au substrate and a Pt foil for 20 min in a 1.6 m.mol.L^{-1} Bi_2O_3 + 0.5 mol.L^{-1} H_2SO_4 solution. The voltammogram registered from this electrode was similar to that of Bi NPs.[19]

In situ FTIR

In situ infrared experiments were performed in a three electrodes glass cell using a polycrystalline Pt disk, a RHE and an Au wire as the counter electrode. A Nexus 8700 (Thermo Scientific) spectrometer equipped with a MCT-A detector and a wire grid ZnSe polarizer (Pike Tech) was the instrument used. The cell was equipped with a CaF_2 (IRRAS) window beveled at 60º and placed at the top of a Veemax (Pike Tech.) reflectance accessory. All the interferograms were collected with a resolution of 8 cm^{-1} and are presented in absorbance units (a.u.) as $-\log(R/Ro)$, where R and Ro represent, respectively, the reflectivity at the sample and reference potentials. Thus, positive and negative bands correspond, respectively, to gain or loss of species with respect to the reference potential. Dynamic experiments (rapid scan-RS) were carried out and the spectra were collected in a rapid scan mode while the electrode potential was swept at 2 mV.s^{-1}. In order to be able to correlate FTIR results with a stable electrochemical response, 9 cycles at 10 mV.s^{-1} were performed prior to the *in situ* experiment. Each spectrum was the average of a set of 260 interferograms which were collected in a 50 mV interval. All the spectra are referred to the reference single beam spectrum collected in the glycerol-containing solutions at 0.10 V.

On line sample collection and High-performance liquid chromatography (HPLC)

A platinum disk (Pt_{disk}) with 0.9 cm diameter was used as the WE, and the experiments were performed using the hanging meniscus configuration.

Samples were collected using a Shimadzu sample collector FRC – 10A by placing a PEEK capillary as close as possible to the WE surface, held at place by a Teflon piece. The capillary and the Teflon piece were thoroughly rinsed with ultrapure water prior to immersion into the electrochemical cell. The collection rate was 60 µL.min^{-1}, while the electrochemical potential was scanned at 1 mV.s^{-1}. Thus, each sample corresponds to a 60 mV potential interval when compared to the voltammogram. The samples travel for 7 min in the peek capillary until reaching the 0.5 mL eppendorf tubes, containing 20 µL of a 0.34 mol.L^{-1} of H_2SO_4 solution in order to reduce the pH of the sample to 2, to avoid the Cannizaro's reaction between aldehydes and alcohols.[20] In order to be able to correlate HPLC results with a stable electrochemical response, 9 cycles at 10 mV.s^{-1} were performed prior to the sample collection.

HPLC experiments were performed in an Agilent series 1200 chromatograph, with a quaternary pump, a thermostatted column compartment, ALS autosampler, vacuum degasser and a refractory index detector kept at 35°C. Three columns were used in series (Aminex HPX87-H + two Shodex Sugar SH1011) and kept at 85°C. The pre-column used was a Bio-Rad 1250131. The mobile phase was 0.5 m.mol.L^{-1} H_2SO_4, with a flow rate of 0.6 mL.min^{-1}. The injected volume was 20 µL.

Chemicals

All solutions were made with ultrapure water (18.2 MΩ cm^{-1}, 25ºC, Millipore), and the chemicals were used without any prior purification. The chemicals used were sulfuric acid (ISO grade, Merck Emsure®), nitric acid (p. a. ACS, LS Chemicals), hydrochloric acid (p. a. ACS, Vetec Chemistry), glycerol (ACS grade, Sigma-Aldrich), bismuth (III) oxide (ReagentPlus®, Sigma-Aldrich) and sodium hydroxide (semiconductor grade, 99.99% trace metal basis, Sigma-Aldrich).

RESULTS

Electrochemical results.

Figure 1A shows a continuous increase in the current density with the Bi coverage (θ_{Bi}) of the Pt_p. However, when Pt_p-Bi electrodes are cycled, the activity decreases continuously. It is well-known that Pt electrodes suffer poisoning due to the irreversible adsorption of intermediates of the EOG.[21–25] Besides, figure S1 show that even if the electrode coverage is not affected by the electrochemical cycling, there is some rearrangement of the surface atoms that compromises the electrodes activity.

A more stable response can be obtained by adding a Bi atoms supply to the solution. Thus, we modify the surfaces *in situ* by cycling the electrodes in a solution containing 0.1 mol.L^{-1} NaOH + 0.1 mol.L^{-1} GlOH + 10^{-x} mol.L^{-1} Bi_2O_3 (x = 8, 7, 6, 5 and 4). Figure 2 show the impact of the presence of Bi ions in solution on the EOG. Varying systematically the concentration of the ions we get a broad range of θ_{Bi} starting from partially (x = 8, 7) to completely (x = 6 and 5) covered electrodes and also including a response similar to that of a bulk Bi electrode (x = 4) (For a detailed discussion see figures S2, S3, S4 and S5).

To understand the promotion of the EOG by the Bi adatoms and to study possible changes in the selectivity of the reaction we performed *in situ* FTIR and HPLC *on line* studies in: i) 0.1 mol.L^{-1} NaOH + 0.1 mol.L^{-1} GlOH and ii) 0.1 mol.L^{-1} NaOH + 0.1 mol.L^{-1} GlOH +10^{-5} mol.L^{-1} Bi_2O_3 (which is the optimal Bi concentration for the EOG in terms of current density and peak current potential (figure S5).

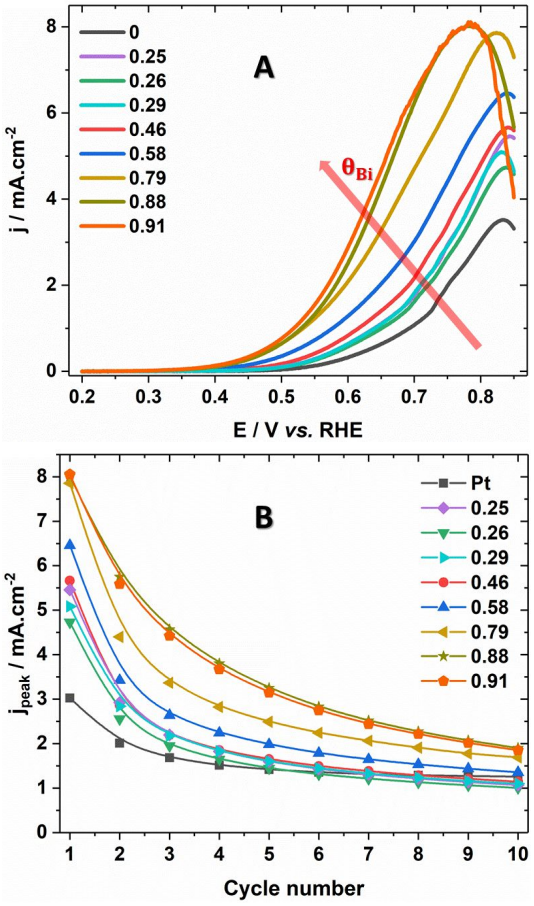

Figure 1. Positive-going sweep of the 1st cycle of the voltammetric response for EOG in 0.1 mol.L^{-1} NaOH + 0.1 mol.L^{-1} GlOH on Pt with several θ_{Bi}. Sweep rate of 10 mV.s^{-1} (A). Peak current density (j_{peak}) *vs* cycle number for selected values of θ_{Bi} (B). Data in figure B was extracted from figure A.

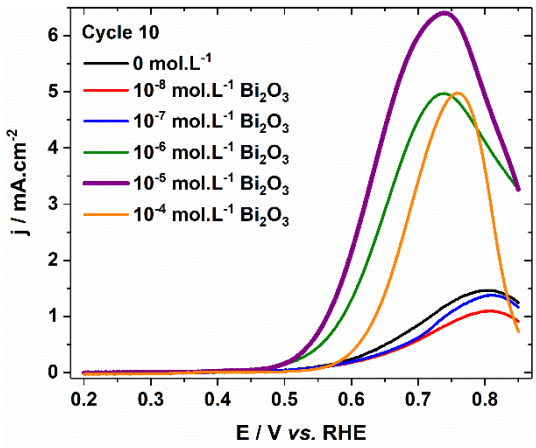

Figure 2. Positive-going sweep of the 10th cycle of the voltammetric response for EOG in 0.1 mol.L^{-1} NaOH + 0.1 mol.L^{-1} GlOH + 10^{-x} mol.L^{-1} of Bi_2O_3 on Pt. Sweep rate of 10 mV s^{-1}.

In situ FTIR

Figure 3 shows FTIR spectra obtained between 0.10 and 0.85 V for Pt_p and Pt_p-Bi (10^{-5} mol.L^{-1} of Bi_2O_3) using deuterated water (D_2O). Both series of spectra show the following features: i) a band at ≈1400 cm^{-1} due to presence of carbonate (CO_3^{2-}) ions (figure S7), ii) a band at ≈1590 cm^{-1} assigned to the stretching mode of the COO^- group,[7,26,27] and iii) a band at 1730 cm^{-1} due to a C=O (carbonyl group) stretching.[28,29] The broad band at 1642 cm^{-1}, corresponding to HOH stretching mode of water,[26,30] is suppressed in these spectra due to the substitution of H_2O (Figure S6) by D_2O.

Figure S7 shows ATR spectra obtained in 0.1 mol.L^{-1} NaOH solution for several possible products of the EOG. Mesoxalate, glycerate and formate show intense bands at ≈1590 cm^{-1}, making them the most likely candidates to be responsible for the band observed in our spectra at this frequency. Several products (tartronate, oxalate, glyoxylate and glycolate) present a band at ≈1730 cm^{-1} together with another intense one at lower frequencies, i.e. at ≈1630 cm^{-1} for tartronate and oxalate and ≈1590 cm^{-1} for glyoxylate and glycolate. The band at ≈1630 cm^{-1} is not present in our spectra, permitting us to rule out the products tartronate and oxalate. Importantly, DHA also presents a feature at ≈1730 cm^{-1} and other at ≈1400 cm^{-1} overlapping the carbonate band. Thus, DHA, glyoxylate and glycolate are the most suitable candidates to be responsible for the feature at ≈1730 cm^{-1} in figure 3, once that their corresponding bands at ≈1590 cm^{-1} would be superimposed to the intense band of glycerate, mesoxalate and/or formate.

The region bellow 1300 cm^{-1} is difficult to analyze due to the superimposition of bands from several compounds. Unfortunately, glyceraldehyde only shows intense bands in this crowded region, making its identification by FTIR almost impossible.

Even if we observe similar features for both systems, the simple inspection of the figure 3 allows us to conclude that the adsorption of Bi highly decreases the ratio [CO_3^{2-}]/[glycerate/mesoxalate/formate] (band at 1400 cm^{-1} /band at 1590 cm^{-1}).

Another important difference between the systems appears between 1800 cm^{-1} and 2100 cm^{-1}. Pt_p shows a set of bands centered at 1850 cm^{-1} and 2040 cm^{-1}, due to the presence of bridge bonded and linearly bonded CO, respectively. In contrast, they are absent for Pt_p-Bi, as observed in other contributions.[8,11,14]

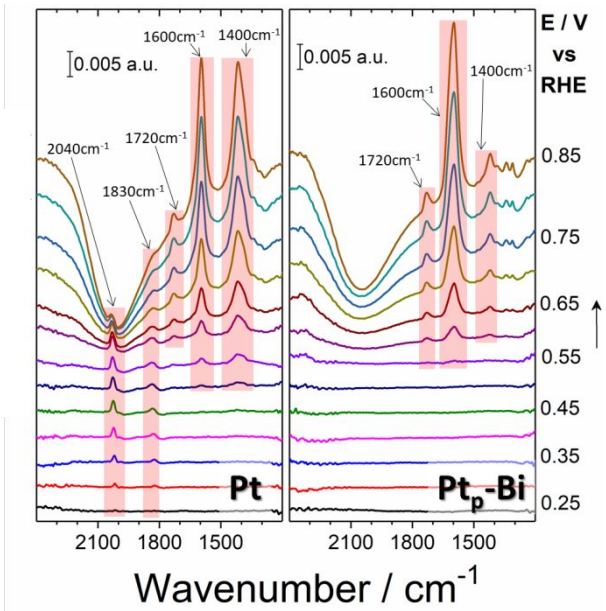

Figure 3. FTIR spectra obtained in 0.1 mol.L^{-1} NaOH + 0.1 mol.L^{-1} GlOH (Pt_p) and 0.1 mol.L^{-1} NaOH + 0.1 mol.L^{-1} GlOH + 10^{-5} mol.L^{-1} of Bi_2O_3 (Pt_p-Bi).

HPLC on line

Figure 4 shows the linear positive sweep recorded during the sample collection (A and B) and the concentration of the products detected during the potential scanning as a function of the electrode potential (C and D). These data were extracted from the chromatograms showed in figure S8, the chromatograms for the standards (figure S9) and the calibration curves (figure S10).

The results in figure 4 (A and B) are qualitatively the same than those in figure 2. Differences appeared due to the differences in the sweep rate, which was 1 $mV.s^{-1}$ during the HPLC *on line* experiment, and to the fact that figure 2 shows results obtained during a continuous cycling. On the other hand, before starting the sample collection it is necessary to stop the scan for tip positioning.

It is worth noting that whereas only relatively low concentrations of glycerate were detected with Pt_p, the concentration of glycerate significantly increases (about 5-6 times) in the presence of Bi. These results strongly support the assignment of the FTIR band at 1590 cm^{-1} to glycerate. Besides, we also detected the presence of glycolate and formate at potentials higher than 0.75V for Pt_p-Bi. Thus, HPLC results support the assignment of the band observed at 1730 cm^{-1} for Pt_p-Bi to glycolate (glyoxylate was not detected). Even if it is likely that the band observed for the system Pt_p at 1730 cm^{-1} also belongs to glycolate, we cannot assure it because the molecule was not detected by HPLC, probably because its concentration was under the resolution limit (50 $\mu mol.L^{-1}$). Actually, a closer inspection of the chromatogram at 0.85 V seems to show a very low intensity band due to this molecule.

Figures S11 and S12 show that both, DHA and glyceraldehyde, are not stable in alkaline media. Thus, our collection method is not able to detect these molecules. We detected glycolate with Pt_p-Bi. Thus, the low intense band at ≈1730 cm^{-1} can be justified, at least in part, due to the presence of this product. Therefore, if DHA is generated, its concentration must be low, and as shown in figures S11 and S12 it will be quickly converted to glycerate. For Pt_p, the analysis is even more difficult due to the extremely low production of glycolate, DHA or both.

HPLC results also show that the band at ≈1590 cm^{-1} arises due to the superimposition of those for glycerate and formate. The comparison between the development of the FTIR band in figure 4F and the concentration profiles obtained by HPLC *on line*, suggest that the FTIR band emerges as a consequence of the production of glycerate at low potentials (below 0.8 V) and have contribution from both molecules at higher potentials. We cannot make the same analysis for the case of Pt_p, because at concentrations ≈10 $\mu mol.L^{-1}$ it is not possible to accurately integrate the band which is close to the detection limit (figure S8).

DISCUSSION

In this work, we showed that the adsorption of Bi on Pt_p promotes the EOG and that the activity of the electrode continuously augments increasing θ_{Bi}. However, we also conclude that the surface slightly rearranges when cycled between 0.20 and 0.85 V in the presence of glycerol (figure S1).

By plotting the current densities obtained in figure 1 vs. θ_{Bi} for several electrochemical potentials (figure S13) we found an exponential relationship. This dependence, which becomes more pronounced at higher potentials, indicates that Bi atoms act not only by preventing the GlOH adsorption on Pt (third body effect),[31–33] but also modifying the adsorption energies of Pt and the adsorbates (electronic effect).

By directly adding different quantities of Bi_2O_3 to the solution containing 0.1 $mol.L^{-1}$ NaOH + 0.1 $mol.L^{-1}$ GlOH, we were able to obtain not only stable Bi-modified Pt surfaces with several θ_{Bi}, but also highly active surfaces for the EOG, displaying higher currents densities in a broader potential window than those observed in absence of Bi.

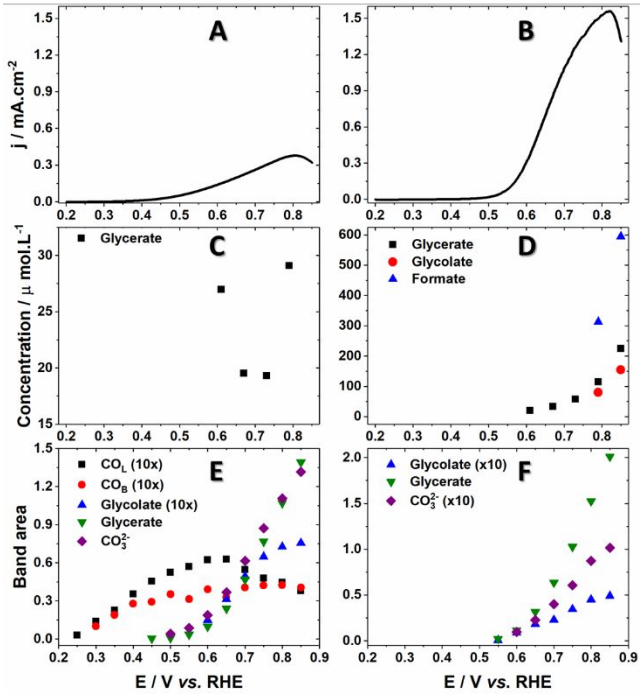

Figure 4. Positive-going sweep of the EOG in 0.1 $mol.L^{-1}$ NaOH + 0.1 $mol.L^{-1}$ GlOH + 10^{-5} $mol.L^{-1}$ of Bi_2O_3 for Pt_p (A) and Pt_p-Bi (B). Sweep rate of 1 $mV.s^{-1}$. (C) and (D) show the concentration of different products *vs*. the electrochemical potential determined using HPLC *on line*, for Pt_p and Pt_p-Bi, respectively. (E) and (F) where obtained by integrating the corresponding bands in figure 3 for Pt_p and Pt_p-Bi, respectively. Some of the bands areas were multiplied by an arbitrary value to show all the results in the same scale.

In situ FTIR results also show relevant information about C-C bond breaking. The ratio $[CO_3^{2-}]$/[Glycerate] is much higher in absence than in presence of Bi, indicating that the adatoms prevent the C-C bond breaking. However, the presence of formate and glycolate (HPLC *on line*), undoubtedly detected at potential higher than 0.8 V by HPLC, showed that this C-C bond breaking hindering also depends on the electrode potential.

Thus, the combination of *in situ* FTIR and HPLC *on line* suggests that the anodic currents observed in figure 4 (A and B) are mainly due to the complete oxidation of GlOH to CO_3^{2-} and to Glycerate in Pt_p and to Glycerate, Formate and Glycolate in Pt_p-Bi. We cannot discard the presence of DHA, but, as discussed before, if it is produced, its concentration must be low.

Regarding the DHA, we want to call the reader's attention to the lack of stability of the molecule in alkaline media (figure S11 and S12). Surprisingly, there are plenty of articles claiming high concentration of the molecule even in solutions more alkaline that ours.

It is worth noting that the addition of Bi results in an increase of activity of about 5-6 times (in terms of current density) compared to that observed in its absence. Additionally, the fact that HPLC *on line* shows that the production of glycerate also increases by 5-6-fold, is a strong evidence that the incorporation of Bi also

induces a modification in the selectivity and, particularly, the selectivity towards glycerate is clearly enhanced.

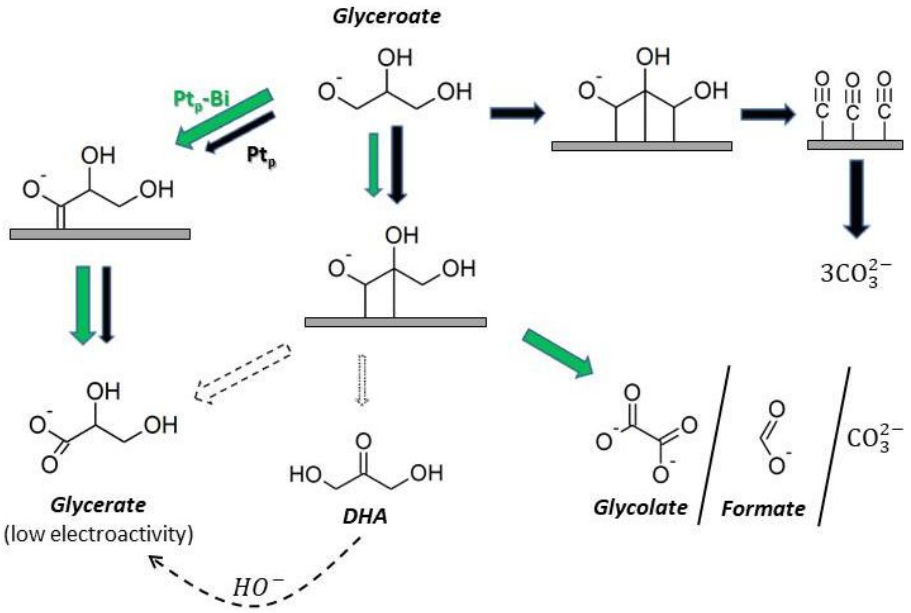

Figure 5: Reaction pathways for the EOG on Pt_p and Pt_p-Bi. The link between the reactant, intermediates and product was done including some hypothetical, non-experimentally determined intermediates (except for CO). The glyceroate ion is in equilibrium with glycerol in solution. We did not include GlOH as a reactant as it is far less reactive than the anion.

We have unraveled the effect of Bi adatoms on the activity and selectivity of the EOG. The *in situ* techniques permit us to rationalize the activities of the electrodes in terms of the reaction products and the formation of adsorbed CO.

Based on the intermediates proposed by Garcia et. al.[34] for the EOG in acidic media, and that it is accepted that the higher currents observed in alkaline media are due to a higher reactivity of the deprotonated glycerol (glyceroate ion),[35] we hypothesize the reaction mechanism showed in figure 5.

In our proposal, glyceroate can bind to the surface through one, two or three carbons (it may happen in one or several steps, especially for the case of the triple bonded intermediate). Pt_p favors the formation of multiple bonded intermediates and Pt_p-Bi forms mainly single bonded intermediates due to a steric effect. Thus, multiple bonded intermediates are favored by the availability of neighboring Pt sites, a situation of lower probability in our experimental conditions, where Pt_p is covered by adatoms.

The triple bonded intermediate, only present in Pt_p, suffers mainly a complete C-C bond breaking (very likely in several reaction steps) to produce adsorbed CO, which then is oxidized to CO_3^{2-}. On the other hand, the intermediated bonded with one carbon atom is present in both electrodes. The fact that the formation of glycerate is much higher in Pt_p-Bi than in Pt_p indicates that this intermediate reacts faster in presence of Bi or that it is formed in higher amounts in this surface, or both options are happening at the same time. In other contributions,[34,36,37] it was hypothesized that Bi stabilizes similar intermediates to what we propose, through an interaction between the oxygen of the intermediates with the Bi adatoms.[14,37] It is important to note that we postulate an intermediate bonded through both the primary and secondary carbon. Garcia et. al.[34] postulated that it could act as a precursor of glyceric acid and DHA (in acid media). In alkaline media, this kind of selectivity is not observable, once that DHA quickly degrades, forming glycerate, which is a dead end in the electrooxidation pathway due to its low electroactivity compared to glyceroate, which is present in much higher concentrations (figure S14).

Finally, at higher potentials, glycolate, formate and carbonate were observed on Pt_p-Bi. The generation of products through C-C bond breaking justifies the presence of a multiple bonded intermediate in this catalyst.

CONCLUSION

In this paper we found that the Bi-decorated Pt surface rearranges in alkaline solution when the electrode is cycled between 0.2 V and 0.85 V in presence of glycerol. We stabilize the oxidation currents by adding Bi ions to the electrolyte, and found that 10^{-5} mol.L^{-1} is the optimal ion concentration.

The activity of Pt_p increases by about fivefold when the optimal quantity of Bi ions is added to the solution. Besides, the adatom strongly impacts the reaction products by suppressing the pathways with C-C bond breaking, hindering the formation of CO (and other unknown intermediates) and enhancing the production of Glycerate.

The adsorption of Bi on Pt_p enhances the production of glycerate in alkaline media and of DHA in acid media. Besides, the peak current recorded at 1mV.s^{-1} in this work was one order of magnitude higher than that obtained in acid media.

ASSOCIATED CONTENT

Supporting Information.

Cyclic voltammetry experiments in 0.1 mol.L^{-1}NaOH +0.1 mol.L^{-1}GlOH + 10^{-5}mol.L^{-1} Bi_2O_3 .Cyclic voltammetry experiments in 0.1 mol.L^{-1} NaOH + 10^{-5} mol.L^{-1} of Bi_2O_3. Similar results to those of figure 3, but in water. ATR spectra of possible products in 0.1 mol.L^{-1} NaOH. Chromatograms obtained analyzing the samples of

the technique HPLC *on line*. Chromatograms of possible products. Calibration curves for the determination of the concentration of the products detected in this work. Stability tests for glyceraldehyde and DHA in alkaline media.
This information is available free of charge on the ACS Publications website

AUTHOR INFORMATION

Corresponding Author

* email: pablosf@unicamp.br (P.S.F)

ACKNOWLEDGMENT

Financial support from the Brazilian agencies: PSF and JLB thanks FAPESP (grants: 2016/01365-0) and Shell and the strategic importance of the support given by ANP (Brazil's National Oil, Natural Gas and Biofuels Agency) through the R&D levy regulation. MBCS thanks PRP-FAEPEX and RAV and VYY thanks SAE-Unicamp for their scholarships.
J.S-G. acknowledges financial support from VITC (Vicerrectorado de Investigación y Transferencia de Conocimiento) of the University of Alicante (UATALENTO16-02).

REFERENCES

(1) Martins, C. A.; Fernández, P. S.; Camara, G. A. Alternative Uses for Biodiesel Byproduct: Glycerol as Source of Energy and High Valuable Chemicals. In *Increased Biodiesel Efficiency*; Trindade, M., Ed.; Springer: Cham, 2018; pp 159–186.

(2) Dodekatos, G.; Schünemann, S.; Tüysüz, H. Recent Advances in Thermo-, Photo-, and Electrocatalytic Glycerol Oxidation. *ACS Catal.* **2018**, *8*, 6301–6333.

(3) Coutanceau, C.; Baranton, S. Electrochemical Conversion of Alcohols for Hydrogen Production: A Short Overview. *Wiley Interdiscip. Rev. Energy Environ.* **2016**, *5*, 388–400.

(4) Simões, M.; Baranton, S.; Coutanceau, C. Electrochemical Valorisation of Glycerol. *ChemSusChem* **2012**, *5*, 2106–2124.

(5) de Souza, M. B. C.; Fernández, P. S.; Solla-Gullón, J. Adatom Decorated Shape-Controlled Metal Nanoparticles: Advanced Electrocatalysts for Energy Conversion. *Curr. Opin. Electrochem.* **2018**, *9*, 121–128.

(6) Angelucci, C. A.; Souza-Garcia, J.; Fernández, P. S.; Santiago, P. V. B.; Sandrini, R. M. L. M. Glycerol Electrooxidation on Noble Metal Electrode Surfaces. In *Encyclopedia of Interfacial Chemistry*, 1; Wandelt, K., Ed.; Eslevier: New York, 2018; Vol. 5.2, pp. 643-650.

(7) Simões, M.; Baranton, S.; Coutanceau, C. Electro-Oxidation of Glycerol at Pd Based Nano-Catalysts for an Application in Alkaline Fuel Cells for Chemicals and Energy Cogeneration. *Appl. Catal. B Environ.* **2010**, *93*, 354–362.

(8) Simões, M.; Baranton, S.; Coutanceau, C. Enhancement of Catalytic Properties for Glycerol Electrooxidation on Pt and Pd Nanoparticles Induced by Bi Surface Modification. *Appl. Catal. B Environ.* **2011**, *110*, 40–49.

(9) Zalineeva, A.; Baranton, S.; Coutanceau, C. How Do Bi-Modified Palladium Nanoparticles Work towards Glycerol Electrooxidation? An in Situ FTIR Study. *Electrochim. Acta* **2015**, *176*, 705–717.

(10) Kwon, Y.; Hersbach, T. J. P.; Koper, M. T. M. Electro-Oxidation of Glycerol on Platinum Modified by Adatoms: Activity and Selectivity Effects. *Top. Catal.* **2014**, *57*, 1272–1276.

(11) Kwon, Y.; Birdja, Y.; Spanos, I.; Rodriguez, P.; Koper, M. T. M. Highly Selective Electro-Oxidation of Glycerol to Dihydroxyacetone on Platinum in the Presence of Bismuth. *ACS Catal.* **2012**, *2*, 759–764.

(12) Kimura, H.; Tsuto, K.; Wakisaka, T.; Kazumi, Y.; Inaya, Y. Selective Oxidation of Glycerol on a Platinum-Bismuth Catalyst. *Appl. Catal. A, Gen.* **1993**, *96*, 217–228.

(13) Caneppele, G. L.; Almeida, T. S.; Zanata, C. R.; Teixeira-Neto, É.; Fernández, P. S.; Camara, G. A.; Martins, C. A. Exponential Improving in the Activity of Pt/C Nanoparticles towards Glycerol Electrooxidation by Sb Ad-Atoms Deposition. *Appl. Catal. B Environ.* **2017**, *200*, 114–120.

(14) Garcia, A. C.; Birdja, Y. Y.; Tremiliosi-Filho, G.; Koper, M. T. M. Glycerol Electro-Oxidation on Bismuth-Modified Platinum Single Crystals. *J. Catal.* **2017**, *346*, 117–124.

(15) Kahyaoglu, A.; Beden, B.; Lamy, C. Oxydation Electrocatalitique Du Glycerol Sur Electrodes d ' or et de Platine En Milieu Aqueux. *Electrochim. Acta* **1984**, *29*, 1489–1492.

(16) Kwon, Y.; Schouten, K. J. P.; Koper, M. T. M. Mechanism of the Catalytic Oxidation of Glycerol on Polycrystalline Gold and Platinum Electrodes. *ChemCatChem* **2011**, *3*, 1176–1185.

(17) Brimaud, S.; Solla-Gullón, J.; Weber, I.; Feliu, J. M.; Behm, R. J. Formic Acid Electrooxidation on Noble-Metal Electrodes: Role and Mechanistic Implications of PH, Surface Structure, and Anion Adsorption. *ChemElectroChem* **2014**, *1*, 1075–1083.

(18) Clavilier, J.; Feliu, J. M.; Aldaz, A. An Irreversible Structure Sensitive Adsorption Step in Bismuth Underpotential Deposition at Platinum Electrodes. *J. Electroanal. Chem. Interfacial Electrochem.* **1988**, *243*, 419–433.

(19) Van der Horst, C.; Silwana, B.; Iwuoha, E.; Somerset, V. Synthesis and Characterization of Bismuth-Silver Nanoparticles for Electrochemical Sensor Applications. *Anal. Lett.* **2015**, *48*, 1311–1332.

(20) Birdja, Y. Y.; Koper, M. T. M. The Importance of Cannizzaro-Type Reactions during Electrocatalytic Reduction of Carbon Dioxide. *J. Am. Chem. Soc.* **2017**, *139*, 2030–2034.

(21) Martins, C. A.; Giz, M. J.; Camara, G. A. Generation of Carbon Dioxide from Glycerol: Evidences of Massive Production on Polycrystalline Platinum. *Electrochim. Acta* **2011**, *56*, 4549–4553.

(22) Fernández, P. S.; Martins, M. E.; Martins, C. A.; Camara, G. A. The Electro-Oxidation of Isotopically Labeled Glycerol on Platinum: New Information on C-C Bond Cleavage and CO2 Production. *Electrochem. commun.* **2012**, *15*, 14–17.

(23) Fernández, P. S.; Martins, C. A.; Martins, M. E.; Camara, G. A. Electrooxidation of Glycerol on Platinum Nanoparticles: Deciphering How the Position of Each Carbon Affects the Oxidation Pathways. *Electrochim. Acta* **2013**, *112*, 686–691.

(24) Gomes, J. F.; Martins, C. A.; Giz, M. J.; Tremiliosi-Filho, G.; Camara, G. A. Insights into the Adsorption and Electro-Oxidation of Glycerol: Self-Inhibition and Concentration Effects. *J. Catal.* **2013**, *301*, 154–161.

(25) Sandrini, R. M. L. M.; Sempionatto, J. R.; Herrero, E.; Feliu, J. M.; Souza-Garcia, J.; Angelucci, C. A. Mechanistic Aspects of Glycerol Electrooxidation on Pt(111) Electrode in Alkaline Media. *Electrochem. commun.* **2018**, *86* (December 2017), 149–152.

(26) Ferreira, R. S.; Janete Giz, M.; Camara, G. A. Influence of the Local PH on the Electrooxidation of Glycerol on Palladium-Rhodium Electrodeposits. *J. Electroanal. Chem.* **2013**, *697*, 15–20.

(27) González-Cobos, J.; Baranton, S.; Coutanceau, C. A Systematic in Situ Infrared Study of the Electrooxidation of C3 Alcohols on Carbon-Supported Pt and Pt–Bi Catalysts. *J. Phys. Chem. C* **2016**, *120*, 7155–7164.

(28) Fernández, P. S.; Gomes, J. F.; Angelucci, C. A.; Tereshchuk, P.; Martins, C. A.; Camara, G. A.; Martins, M. E.; Da Silva, J. L. F.;

Tremiliosi-Filho, G. Establishing a Link between Well-Ordered Pt(100) Surfaces and Real Systems: How Do Random Superficial Defects Influence the Electro-Oxidation of Glycerol? *ACS Catal.* **2015**, *5*, 4227–4236.

(29) Fernández, P. S.; Tereshchuk, P.; Angelucci, C. A.; Gomes, J. F.; Garcia, A. C.; Martins, C. A.; Camara, G. A.; Martins, M. E.; Da Silva, J. L. F.; Tremiliosi-Filho, G. How Do Random Superficial Defects Influence the Electro-Oxidation of Glycerol on Pt(111) Surfaces? *Phys. Chem. Chem. Phys.* **2016**, *18*, 25582–25591.

(30) Schnaidt, J.; Heinen, M.; Denot, D.; Jusys, Z.; Jürgen Behm, R. Electrooxidation of Glycerol Studied by Combined in Situ IR Spectroscopy and Online Mass Spectrometry under Continuous Flow Conditions. *J. Electroanal. Chem.* **2011**, *661*, 250–264.

(31) Climent, V.; García-Arez, N.; Feliu, J. M. Clues for the Molecular-Level Understanding of Electrocatalysis on Single-Crystal Platinum Surfaces Modified Byp-Block Adatoms. In *Fuel Cell Catalysis*; Koper, M. T. M., Wieckowski, A., Eds.; John Wiley & Sons, Inc.: Hoboken, NJ, USA, 2008; pp 209–244.

(32) Herrero, E.; Fernandez-Vega, A.; Feliu, J. M.; Aldaz, A. Poison Formation Reaction from Formic Acid and Methanol on Pt(111) Electrodes Modified by Irreversibly Adsobed Bi and As. *J. Electroanal.Chem* **1993**, *350*, 73–88.

(33) Clavilier, J.; Femandez-Vega, A.; Feliu, J. M.; Aldaz, A. Heterogeneous Electrocatalysis on Well Defined Platinum Surfaces Modified by Controlled Amounts of Irreversibly Adsorbed Adatoms. Part III. Formic Acid Oxidation on the Pt(100)-Bi System. *J. Electroanal. Chem. Interfacial Electrochem.* **1989**, *261*, 113–125.

(34) Garcia, A. C.; Kolb, M. J.; Van Nierop Y Sanchez, C.; Vos, J.; Birdja, Y. Y.; Kwon, Y.; Tremiliosi-Filho, G.; Koper, M. T. M. Strong Impact of Platinum Surface Structure on Primary and Secondary Alcohol Oxidation during Electro-Oxidation of Glycerol. *ACS Catal.* **2016**, *6*, 4491–4500.

(35) Kwon, Y.; Lai, S. C. S.; Rodriguez, P.; Koper, M. T. M. Electrocatalytic Oxidation of Alcohols on Gold in Alkaline Media: Base or Gold Catalysis? *J. Am. Chem. Soc.* **2011**, *133*, 6914–6917.

(36) Boronat-González, A.; Herrero, E.; Feliu, J. M. Fundamental Aspects of HCOOH Oxidation at Platinum Single Crystal Surfaces with Basal Orientations and Modified by Irreversibly Adsorbed Adatoms. *J. Solid State Electrochem.* **2014**, *18*, 1181–1193.

(37) Ferre-Vilaplana, A.; Perales-Rondón, J. V.; Feliu, J. M.; Herrero, E. Understanding the Effect of the Adatoms in the Formic Acid Oxidation Mechanism on Pt(111) Electrodes. *ACS Catal.* **2015**, *5*, 645–654.

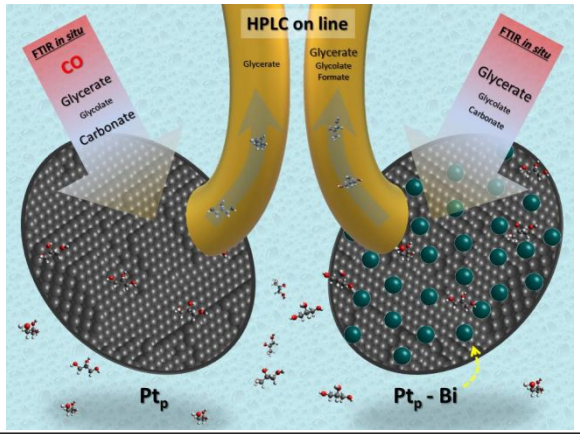
HPLC on line
FTIR in situ
CO
Glycerate
Glycolate
Carbonate
Glycerate
Glycerate
Glycolate
Formate
FTIR in situ
Glycerate
Glycolate
Carbonate
Pt$_p$
Pt$_p$ - Bi